JOURNAL OF AIRCRAFT
Vol. 32, No. 3, May–June 1995

Spectral Mapping of Quasiperiodic Structures in a Vortex Flow

James P. Hubner* and Narayanan M. Komerath†
Georgia Institute of Technology, Atlanta, Georgia 30332

Steady vortex flows over highly swept wings develop quasiperiodic velocity fluctuations. The nature of such fluctuations was explored extensively using a 59.3-deg cropped delta wing at 25-deg incidence in a low-speed wind tunnel. Additional single point tests were conducted over a range of incidences (16–32 deg) and Reynolds numbers (1.2×10^5 to 5.6×10^5) based on the root chord. Cross-spectral analysis of velocity fluctuations, sensed by two hot-wire sensors, was used to track these phenomena to the region of their origin as well as study the evolution and growth of the fluctuations. Results show the existence of narrow, dominant frequency bands containing the majority of the fluctuation energy. At 25 deg the quasiperiodicity originates near the 30% span region and the intensity amplifies downstream as the corresponding peak frequency decreases. Further downstream the frequency levels off while the intensity peaks, then decreases. Coherence trajectory mapping displays a helical path around the core of the vortex system. At a fixed location relative to the model, the product of the Strouhal number and the nominal wake scale was relatively constant with respect to freestream speed.

Nomenclature

b	=	wingspan
b'	=	local wingspan
c	=	wing root chord
f	=	frequency in cycles per second
$G(n)$	=	nondimensional autospectral density
H	=	vertical distance above delta wing surface in tunnel coordinates
mac	=	mean aerodynamic chord
N	=	number of time-domain values per sample block
n_l	=	Strouhal-scaled/reduced frequency, fl/U_∞, based on characteristic length, l
Re	=	Reynolds number
$S(n)$	=	nondimensional cross-spectral density
U_c	=	convection speed
U_∞	=	freestream speed
X, Y, Z	=	tunnel coordinate system, origin fixed to model apex
x', y', z'	=	body coordinate system, origin fixed to model apex
α	=	angle of attack
β	=	projected angle along model surface between the root chord and a ray originating at the apex
$\gamma(n)$	=	nondimensional coherence function
θ	=	projected angle along vertical centerline plane between the model surface and a ray originating at the origin
Λ	=	leading-edge sweep
τ_a	=	time shift to the secondary peak of the autocorrelation

Introduction

THE motivation of this research stems from the tail buffeting problems experienced by swept-wing, twin-tailed aircraft at high angles of attack.[1–5] The best known contributor to this problem is the bursting of strong vortices as on the F/A-18 aircraft[3,4]; however, quasiperiodic velocity fluctuations (almost periodic fluctuations characterized by sharp spectral peaks) have been observed on other configurations, like the F-15, where no strong unburst vortex core is observed.[6] These fluctuations could drive structural modes even where the overall broadband turbulence intensities are quite low.

Background

The flow over a highly swept-winged configuration at high incidence provides many curious phenomena. Such flows are extremely easy to generate in small-scale experiments and have provided surprisingly good representations of phenomena encountered by full-scale flight vehicles, despite large differences in Reynolds number. As such, there is a vast body of literature on vortex flows; Nelson[7] contains a recent survey of literature. However, much remains unknown about the development of velocity fluctuations in a steady vortex flow, except for the intensive research conducted by many organizations on the phenomenon of vortex core bursting. Previous research[6,8–10] regarding the development of quasiperiodic fluctuations in vortex flows over swept-winged aircraft configurations at moderate to high angles of attack has demonstrated that these fluctuations amplify and focus their energy into a narrow frequency band as they move downstream. Every swept-wing configuration tested to date, including generic wing-bodies and isolated delta wings, exhibits this phenomenon. Rediniotis et al.[11] studied the nature of vortex shedding over highly swept delta wings at incidences of 35 deg and higher. Results show that fundamental frequencies develop for simultaneous and alternate shedding. They also describe unassociated spectral peaks detected in unsteady surface pressure measurements that originate further upstream with increasing angle of attack. At incidences studied in our investigation, vortex shedding does not occur and is not an issue; however, the quasiperiodic nature is similar to the peaks characterized by the surface pressure measurements.

Komerath et al.[6] discuss two different mechanisms about the nature of tail vibrations: 1) the structure responds to critical frequencies in the overall broadband spectra and 2) the structural response occurs when a dominant frequency of the flow fluctuation energy coincides with structural modes, even when the overall broadband intensity is low. Figure 1 (from Ref. 6) shows F-15 model and flight test data of flow and structural fluctuations near and on the vertical fin (α = 20 deg). The Strouhal number based on the freestream velocity

Presented as Paper 93-2914 at the AIAA 24th Fluid Dynamics Conference, Orlando, FL, July 6–9, 1993; received Feb. 27, 1994; revision received Aug. 6, 1994; accepted for publication Aug. 30, 1994.

*ONR Graduate Fellow. Student Member AIAA.
†Professor, School of Aerospace Engineering. Associate Fellow AIAA.

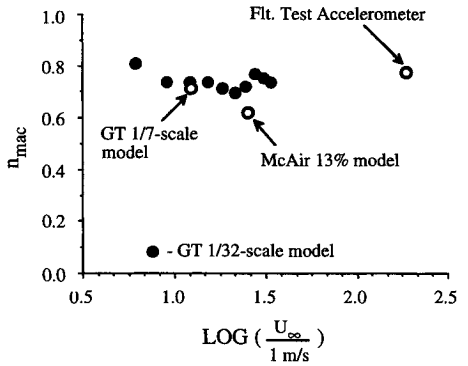

Fig. 1 Strouhal-scaling summary of dominant spectral peak for F-15 models and aircraft at α = 20 deg.

and the mean aerodynamic chord is approximately constant over a wide range of freestream velocities, although the Reynolds number and Mach number are very different over the range of conditions tested. This suggests a flow-structure interaction similar to the second mechanism described. Further insight on the developmental characteristics of the quasiperiodic fluctuations would assist in control techniques to alleviate fin buffeting.[12,13]

Objectives

The origin and evolution of the quasiperiodic fluctuations are the subjects of this article. Although the previous work focused on aircraft and wing-body configurations, this is the authors' first systematic investigation of such fluctuations over an isolated delta wing. The objectives of the investigation were as follows: 1) quantify spectral characteristics of velocity fluctuations over the delta wing, 2) determine the origin or region responsible for the generation of the quasiperiodicity, 3) characterize growth rate and trajectory features, and 4) characterize convection speeds of the quasiperiodic structures.

Experimental Method

Facility and Test Model

For the experiments reported in this article, a cropped delta wing with beveled edges was used. All tests on the delta wing were conducted in the low speed wind tunnel at the School of Aerospace Engineering, Georgia Institute of Technology. The open circuit tunnel is equipped with a traversing mechanism and instrumentation to allow for full automation of the hot-wire experiments. The maximum tunnel freestream speed is 21.3 m/s (70.0 ft/s) and the cross-sectional dimensions of the test section are 1.07 by 1.07 m.

Figure 2 shows the planform of the cropped delta wing. The root chord and wingspan of the model are 398 and 386 mm, respectively. The leading-edge sweep is 59.3 deg. The aluminum model has an 18-deg bevel along both the leading and trailing edges. The planform of the delta wing, including the unusual sweep value, were chosen to be geometrically similar to the wing planform of the generic wing-body model previously tested,[9] excluding the forward leading-edge extensions of that model. Figure 3 is a schematic of the experimental setup.

Instrumentation and Analysis

A pair of tungsten hot-wire probes (5 μm diam) were traversed throughout the flowfield to quantify and analyze features responsible for the quasiperiodicity. From each hot-wire signal, one channel acquired the full signal and the other channel measured a bandpass filtered and amplified signal. The high and low pass filter settings were set at 0.1 and 500 Hz, respectively, and the amplification ranged between 5–200. The filtered signals were continually monitored on an

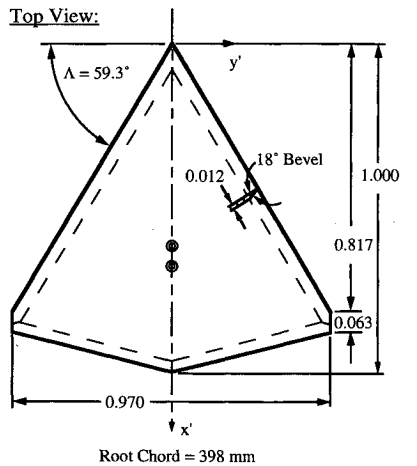

Fig. 2 Planform and dimensions of the delta wing model.

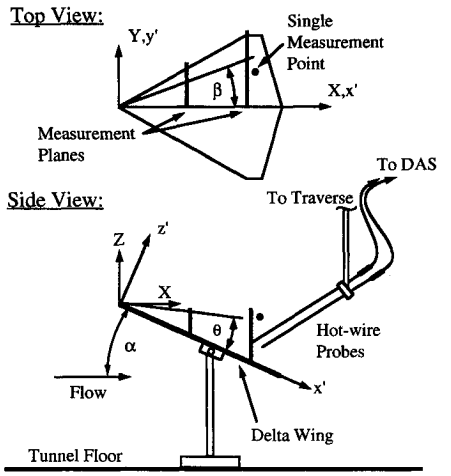

Fig. 3 Experimental setup and measurement locations.

oscilloscope to assist in determining the appropriate amplification for optimum precision.

Signals were digitized in sample blocks of 512 data points using a 16-bit, multichannel, sample-and-hold analog-digital converter. Each digitized block of data was then converted to velocity using the full nonlinear calibration of the sensor and the corresponding value of the unfiltered signal to provide the instantaneous voltage. At each measuring point, up to 200 sample blocks were recorded to calculate a stable ensemble-averaged autospectrum for each signal. Nyquist frequency settings (one-half the sampling frequency) ranged from 256 to 2048 Hz in order to capture a stable peak of the phenomenon as the sensors moved upstream. The corresponding frequency resolution is 1–8 Hz, respectively.

Spectral analysis of the hot-wire signals was used to measure the distribution of the energy contained in the velocity fluctuations as a function of frequency by computing the autospectrum of the velocity fluctuation signal over a discrete frequency range using a standard fast Fourier transform (FFT). The autospectrum indicates the existence of such features as discrete-frequency fluctuations or broadband turbulence. When two fluctuating signals are analyzed, the cross-spectral, cross-correlation, and coherence calculations become of interest. While the cross-spectrum is a measure of energy contained and relative phase between occurrences of fluctuations common to both sensors, the cross-correlation yields how well the two signals are correlated over time. The coherence function between two time series is defined as the ratio of the square of the cross-spectral magnitude to the product of the autospectra within each frequency band,[14] and it is a measure of

linearity over a discrete frequency range between the two signals:

$$\gamma_{12}(n) = \frac{S_{12}(n)^* \cdot S_{12}(n)}{G_1(n) \cdot G_2(n)}$$

This real function of frequency ranges from 1, which indicates perfect linear relationship at that frequency band regardless of time shift, down to 0, which indicates a lack of any linear relationship. Good coherence, approximately 0.5 or higher, can occur even when a substantial time lag exists between the passage of the same fluctuation over two sensors.

Experiments

Due to the symmetry of the flowfield (verified by laser sheet visualization of the vortex systems), all measurements were conducted over the right half of the delta wing. The freestream velocity was 12.2 m/s (40.0 ft/s) and the angle of attack was 25 deg for the extensive flowfield investigation. The hot-wires were aligned perpendicular to the freestream direction for all but one of the experiments. With this alignment, the sensors were sensitive to the streamwise and vertical components of velocity and less sensitive to the lateral component of velocity. Since the focus was on the spectral content of the flowfield, no attempt was made to decompose the three-dimensional flow into its individual components. Probe interference was minimized by using long, thin probes to hold the hot-wires and by staying away from the vortex core. Previous research[6] verified that spectral shapes were minimally affected by probe orientation or probe vibration. The probes were attached to the streamwise and vertical components of the computer controlled traverse.

Vertical planar measurement locations were located at $x'/c = 0.42$ and 0.83, which correspond to the locations previously chosen for detailed planar measurements on the generic wing-body[9] (Fig. 3). The probe holders were aligned perpendicular to the model surface, and the upstream probe was spaced 12.7 mm in front of the downstream probe. The measurement grid spacing inside the two planes were 12.7 and 25.4 mm, respectively. Further measurements were conducted along rays originating from the apex of the wing and passing through specified points downstream, as well as along the leading edge of the delta wing. For the leading-edge surveys, the probe wires were aligned both perpendicular and parallel to the freestream. The parallel alignment was sensitive to the crossflow and vertical fluctuations.

To determine a path that the quasiperiodic structures follow, the sensors were traversed relative to each other. With the downstream probe stationary, the upstream probe was traversed over a vertical grid, 50.8 by 50.8 mm and 23 mm upstream, with measurements acquired on a 25.4 mm grid spacing. Upon completion of the traverse, the downstream probe was moved to the location of the upstream probe's maximum peak magnitude of autospectra while maintaining a high level of coherence. Using this technique, a path of high energy content and high coherence was determined.

A final battery of tests were performed at a single point in the flowfield over a range of angles of attack and freestream speeds (16 to 32 deg and 4.6 to 21.3 m/s, respectively). The measurement point was fixed $z'/c = 0.26$ off the surface at $x'/c = 0.85$ and $y'/c = 0.19$, and was located near the trailing edge and above the vortex core (Fig. 3).

Results and Discussion

Nature of Flowfield

Results from the two vertical measurement planes are presented first. Figures 5a–5d and 6a–6d display the frequency, bandwidth, autospectral intensity, and coherence of the spectral peak in nondimensional form for the upstream and downstream measurement planes, respectively. Frequencies are Strouhal-scaled with the mean aerodynamic chord and freestream speed; the peak spectral intensities are nondimensionalized by the freestream energy $(U_\infty N)^2$. The vertical axis represents the nondimensionalized distance above the model surface, $2H/b$.

Figures 4a and 5a show that peak frequency results in spanwise planar regions decrease downstream and are fairly constant away from the vortex core. Towards the vortex center the peak frequency also decreases. The frequency bandwidth, measured by a 50% decrease of the peak spectral intensity, also broadens near the vortex center (Figs. 4b and 5b). Inspection of the intensity plots (Figs. 4c and 5c) show that the largest gradients in the peak magnitude of the autospectrum are along radial lines directed toward the vortex center. In regions outside the free shear layer roll-up (near the model centerline and just beyond the leading edge), the peak magnitude drops off significantly. The fluctuation intensities are approximately twice as large in the downstream plane as in the upstream plane. Figures 4d and 5d show that the coherence between the signals from the two sensors is relatively high in regions away from the core area. In the upstream plane, coherence values decrease more significantly near the core, distancing the core region as a possible source of the quasiperiodicity. Finally, due to the broader peaks of the coherence function, the coherence value at the frequency corresponding with the autospectral peak of the upstream probe was used.

Figure 6 shows the increase in the autospectral intensity and the corresponding decrease in frequency for the upstream probe as it was traversed downstream along the leading edge. Similar results were obtained from the probe positioned in the crossflow orientation. It is useful to discuss this figure starting at the upstream location ($b'/b = 0.22$), where there is little fluctuation at any frequency. The highest coherence for frequencies above $n = 0.7$ (32 Hz) is 0.14, which is insignificant. At $b'/b = 0.38$, a broadband fluctuation develops over a large frequency range. The coherence at this location increases substantially to 0.57 at $n = 3.3$. At $b'/b = 0.69$ span, amplification and focusing behavior continues. By full span, there is one very sharp and clear peak, with a spectral density 18 times greater than that of the $b'/b = 0.38$ span location, where the fluctuation is first seen. The coherence value at the peak frequency is 0.88. This sequence clearly characterizes the quasiperiodic phenomenon. It shows a small broadband fluctuation developing in a steady vortex flow, then rapidly focusing—shifting frequency—and amplifying into a well-defined narrowband fluctuation. Figure 7 depicts the amplification trend for both sensor orientations: freestream and crossflow. Previously, such phenomena have been observed from measurements made on models of the F-15 aircraft in the context of tail vibrations; here it is seen clearly that the fluctuations originate in the velocity field over a steady, isolated delta wing, and is therefore not always caused by the presence of the tails, fuselage, strakes, engine inlets, forebody shedding, or other details.

Figure 8 shows frequency and growth trends along various rays originating at the apex. For rays A and B, the traversing started at the downstream plane and moved upstream ($\Delta x' = 50$ mm) until no broadband peak was detectable. Ray C_1 was started at the apex and continued downstream ($\Delta x' = 25$ mm). Eventually the peak became disorganized due the proximity of the ray to the vortex core. To continue the investigation downstream, the trajectory was shifted inboard along C_2. The reduced frequency results are similar for all the rays when compared to the measurement location x'/c. This provides further evidence of a near constant frequency over a fixed spanwise location in areas away from the vortex core and suggests a spanwise scaling of frequency. Previous researchers have suggested the local semispan[15] and the turbulent vortex diameter.[16] Results for ray C_2 show that the Strouhal-scaled frequencies level off to a value of 0.9 downstream of the trailing-edge. Growth rates vary along the rays

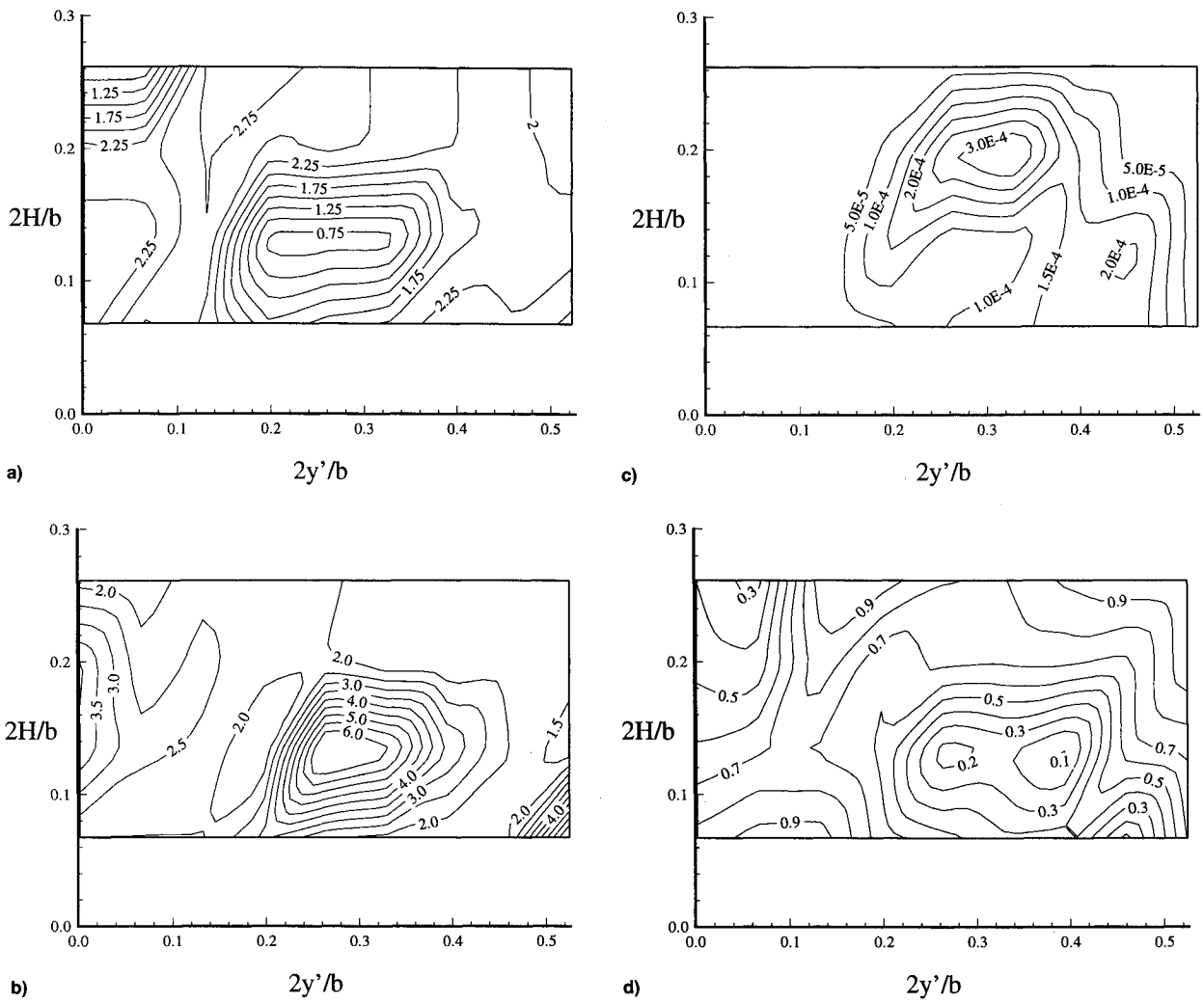

Fig. 4 a) Peak reduced frequency contour n, b) reduced frequency bandwidth contour, c) peak autospectral intensity contour G, and d) peak coherence contour γ: upstream planes.

with the most substantial increase occurring along ray C_1, the path closest to the vortex center trajectory. Downstream of the trailing-edge, the intensity peaks and then decreases along C_2. Coherence values between tandem sensors, configured for rays A and B only, also increased downstream.

Nature of Flow Structures

Figure 9 shows the variation in peak reduced frequency along the leading edge and the corresponding frequency scale calculated from the inverse of the time scale in the autocorrelation function. The time-domain autocorrelation function can be used to measure the time scale of passage of the flow structures over a sensor. Further upstream, the autocorrelation becomes more sharply peaked because of the broadband nature of the fluctuations. As a result, the time scale of correlation measured from this function is shorter, giving a higher value of frequency. Further downstream, the autocorrelation is dominated by the flow structure of interest, so that the time scale is essentially the time scale of the flow structure and the calculated frequency matches that of the spectral peak.

In Fig. 10, the coherence function and the peak autospectral magnitude are used as indicators of the path taken by a given flow structure as it moves downstream. Before the three-dimensional Lagrangian tracking of a flow structure is possible, a means of visualizing the nature of the structure is needed. By following the path of maximum coherence at the peak frequency between the two tandem sensors, one should be able to track the ensemble-averaged trajectory of the flow structure of interest. In implementing this idea, some problems were encountered. First, at the wing trailing edge, there was high coherence over large areas, as seen in Fig. 5d, so that the coherence value was not a sensitive indicator. To overcome this problem, the spectral peak magnitude was used as a second indicator of the path. A second problem was probe interference. An attempt to track a path starting from a location further inboard and below resulted in some nonreliable measurements due to probe interference. Thus, no trajectories could be established originating in lower regions near the centerline.

The results show that the trajectory appears to follow the leading edge and then, starting from point 3, lift into a helical path around the vortex core trajectory (determined via flow visualization). The structures amplify in intensity further downstream in the path, as seen before. The trajectory is fairly stable, in that a survey started at a nearby point in the trailing-edge plane leads roughly along the same path. The initial path along the leading edge is due to the tracking technique from downstream to upstream. Peak spectral intensities decrease rapidly away from the leading edge; thus, when traversing upstream the path of high coherence and intensity will follow the leading edge once it is reached.

The location of the trajectory points are listed in Table 1. Also shown in Table 1 are the convection speeds between two measurement points of Fig. 10. The convection speed was calculated by dividing the probe spacing by the cross-correlation time shift. If no convection speed is shown, then either no time shift was detected or a negative cross-correlation was

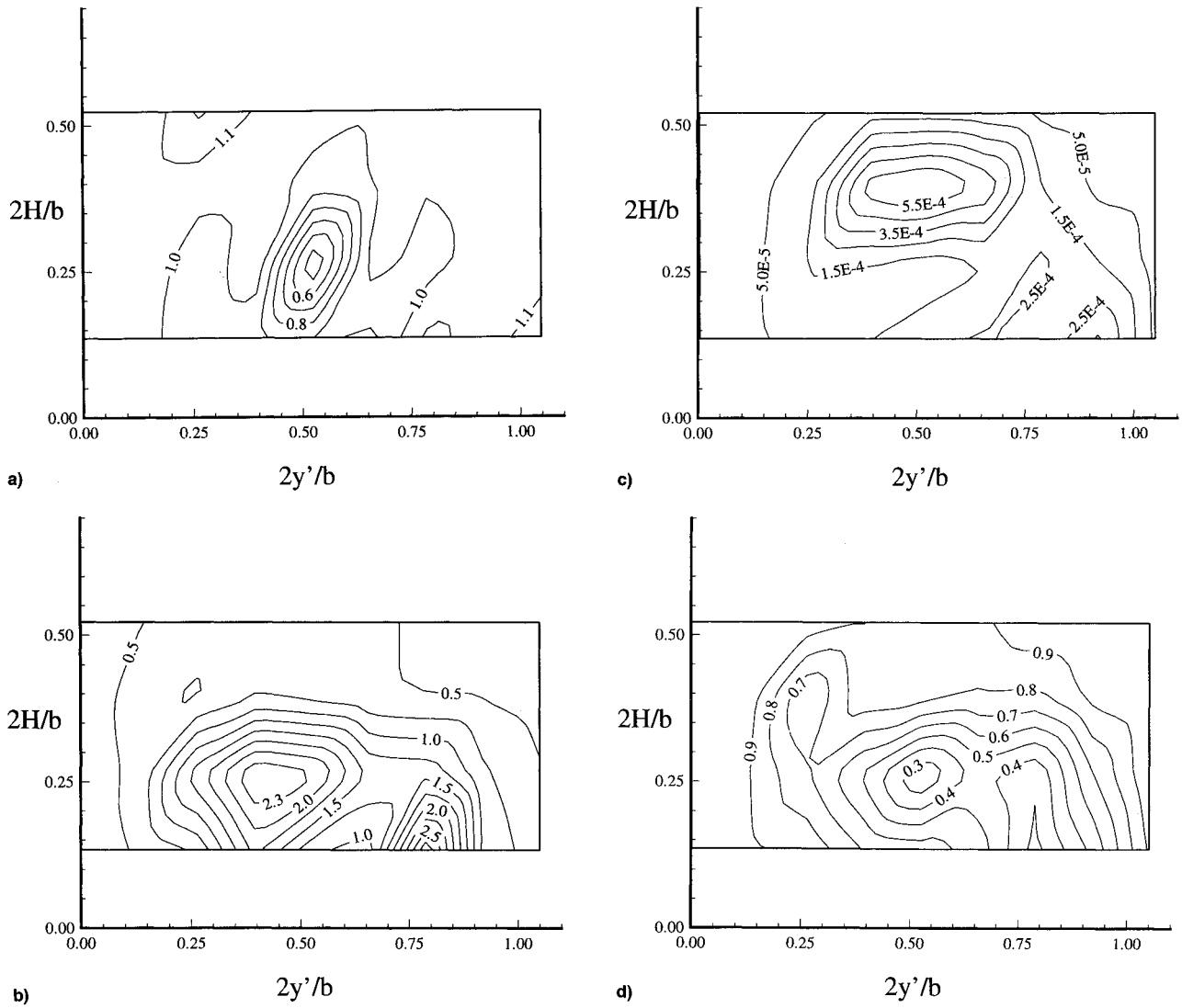

Fig. 5 a) Peak reduced frequency contour n, b) reduced frequency bandwidth contour, c) peak autospectral intensity contour G, and d) peak coherence contour γ: downstream planes.

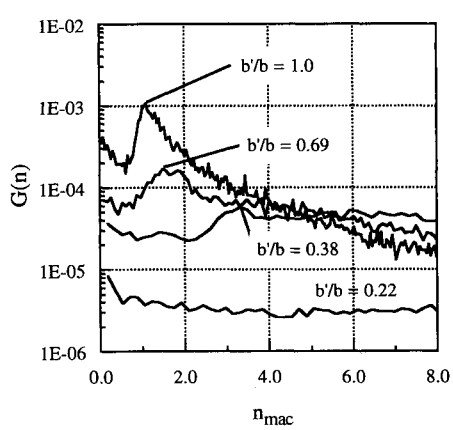

Fig. 6 Autospectral energy distribution along the leading edge: freestream orientation, H = 12.7 mm.

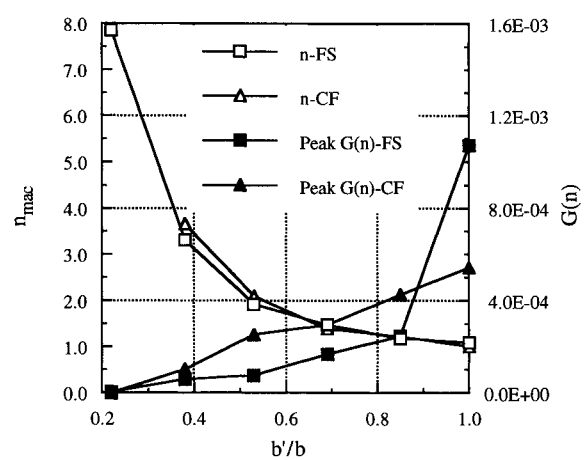

Fig. 7 Reduced frequency and intensity trends of the spectral peak along the leading edge: FS—freestream hot-wire orientation, CF—crossflow hot-wire orientation.

calculated. Convection speed calculations for ray B were 5–6 m/s; however, no time shift was calculated along ray A.

Also shown in Fig. 10 is the origin of the first broadband spectral "hump" detected along different paths. Table 2 lists the origin locations. The quasiperiodic phenomena was detected further upstream near the leading edge than near the root chord. This characteristic might be explained by the helical trajectory convecting the quasiperiodicity inboard towards the centerline. Additional tests at increasing angles of attack showed that the origin along the leading edge moved upstream in correspondence with the breakdown of the primary vortex visualized by Wentz and Kohlman[17] for a delta wing of similar sweep and at a Reynolds number three times

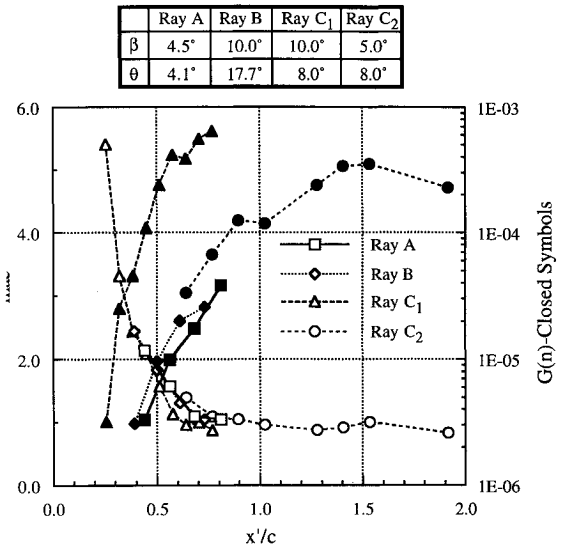

Fig. 8 Reduced frequency and intensity trends of the spectral peak along different ray trajectories.

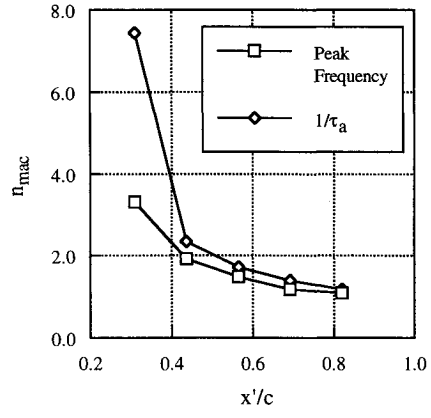

Fig. 9 Comparison between the measured peak frequency and the inverse of the autocorrelation time shift along the leading edge.

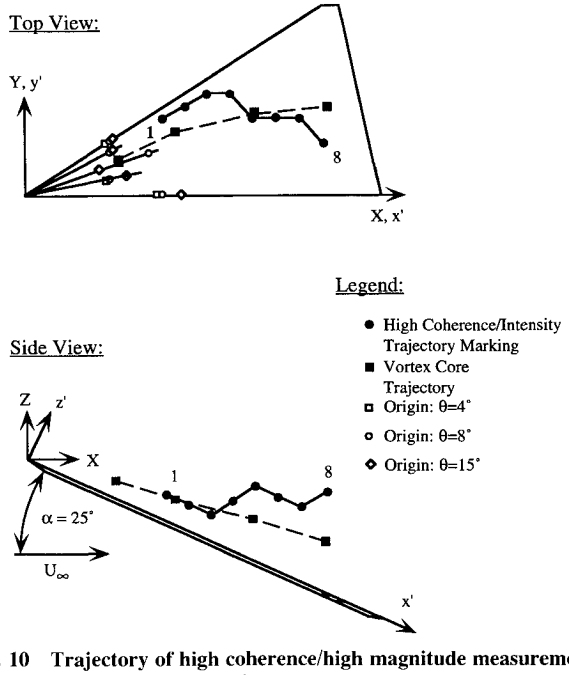

Fig. 10 Trajectory of high coherence/high magnitude measurements and spectral peak origin locations.

Table 1 Location of trajectory points with convection speeds for Fig. 12

Point	x'/c	y'/c	z'/c	H/c	U_c/U_∞
1	0.36	0.19	0.058	0.064	——
2	0.42	0.22	0.058	0.064	0.45
3	0.48	0.26	0.058	0.064	0.43
4	0.52	0.26	0.12	0.13	0.70
5	0.55	0.19	0.17	0.19	0.73
6	0.62	0.19	0.17	0.19	——
7	0.69	0.19	0.17	0.19	1.4
8	0.72	0.13	0.23	0.26	——

Table 2 Location of spectral origin (x'/c) along the rays shown in Fig. 12

	θ = 4 deg	θ = 8 deg	θ = 15 deg
Centerline	0.35	0.35	0.38
β = 10 deg	0.22	0.22	0.26
β = 18.5 deg	0.26	0.32	0.19
β = 26.5 deg	——	0.22	0.22
Leading edge	0.22	0.22	0.22

as high ($Re = 1 \times 10^6$). At incidences of 18, 25, and 30 deg, the first detected spectral humps were at b'/b = 0.85, 0.3, and 0.15, respectively. Breakdown locations were visualized at approximately 0.75, 0.3, and 0.1, respectively. Initial tests on wings of differing sweep showed that decreasing the sweep angle caused the origin move upstream as well.

The origin location results seem to show a relationship between the quasiperiodicity and vortex breakdown, whereas the planar spectral results and trajectory coherence measurements do not. Further investigations[18-23] in the primary shearing regions—the leading edge, the vortex core, and the surface boundary layer—provide additional insight to the mechanisms creating instabilities in the vortex flowfield. Several types of instabilities are discussed among these investigations: discrete vortices emanating from the leading-edge, spatially static structures in the shear layer roll-up, vortex core spiraling, spanwise surface vortices, and surface streakline curvature. Arguments presented in Ref. 22 point to the latter two mechanisms playing a key role in the development of quasiperiodic fluctuations as shown by the Strouhal matching between hot-wire spectral measurements and flow visualization results. As for the role of breakdown, it appears implausible that a core that has become fully turbulent or has broken down into chaotic flow can continue to drive the narrowband phenomenon far downstream of the bursting region. The helical trajectory of measured coherence, the Strouhal-scaling of spectral and flow visualization measurements of the core motion, and the visualized spiral nature of the structure about the core do indicate, however, that the vortex shear region does participate in the process.

Single Point Measurements

Figures 11–13 show peak frequency and intensity trends with respect to increasing incidence and freestream speed. The measurement point, shown in Fig. 3, was chosen to simulate a possible location for a vertical fin. In reference to the vortex core, the measurement location is inboard and above the core. The linear frequency/velocity relationship of the fluctuation is shown in Fig. 11. Increases in incidence causes the Strouhal-scaled frequency to decrease. Previous research[13,24] has shown the Strouhal number is relatively independent of incidence when scaled by $\sin(\alpha)$, a nominal wake scaling factor. Figure 12 displays the $n \sin(\alpha)$ scaling with respect to the freestream Reynolds number. The scaled Strouhal number, based on the local semispan, is relatively constant and independent of Reynolds number (for the range tested). The values ranged between 0.27–0.37.

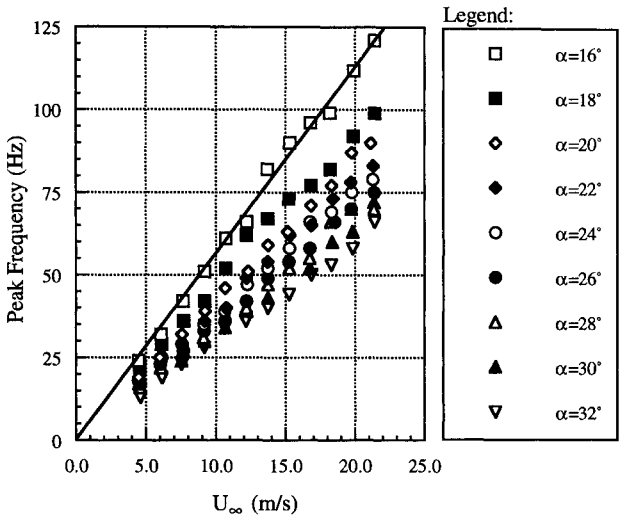

Fig. 11 Variation of peak frequency with freestream speed.

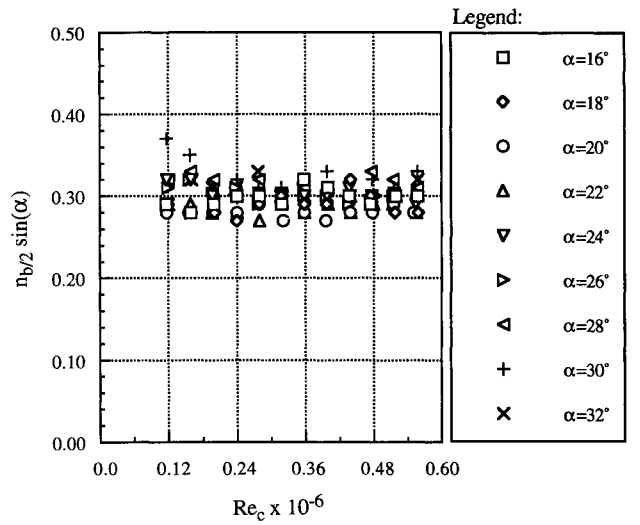

Fig. 12 Variation of scaled Strouhal number with Reynolds number.

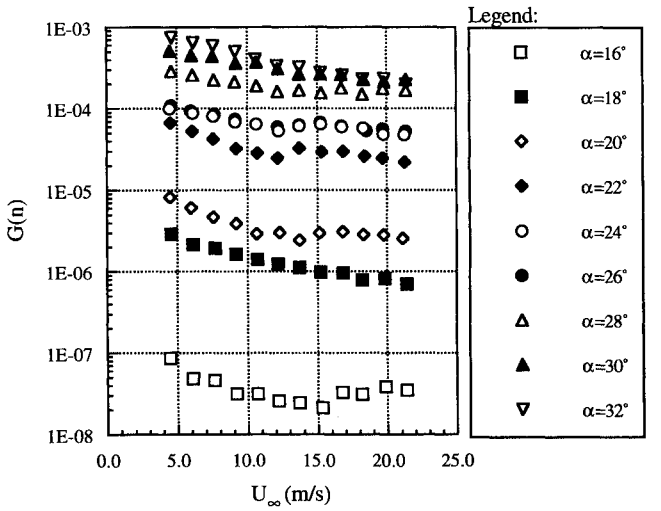

Fig. 13 Variation of peak nondimensionalized autospectral intensity with freestream speed.

Figure 13 is a plot of the nondimensionalized peak spectral energy for the various test conditions. In general, as incidence and freestream speed increase, the absolute spectral energy within the vortex increases, probably an effect of the strengthening shear layer. However, when nondimensionalized by the freestream energy, a general decrease is observed for most incidences. As the angle of attack is increased, the relative intensity increases substantially (four orders of magnitude over the tested range). This trend is amplified by the fixed measurement location. The vortex system is further displaced from the surface for higher incidences; thus, the probe measurements are deeper into the shear layer, recording the higher intensity. The changes in the core position due to changes in the freestream speed do not have as pronounced an effect.

Conclusions

Spectral characteristics of the velocity fluctuations were quantified in planar and trajectory surveys for an isolated, 59.3-deg delta wing at 25-deg angle of attack (U_∞ = 12.2 m/s). The following conclusions are made:

1) Dominant, narrow frequency bands exist in the flowfield where most of the velocity fluctuation energy is contained.

2) The peak spectral intensity increases, peak frequency decreases, and coherence increases over a larger area further downstream in the flowfield. Eventually the intensity decreases and the frequency levels off downstream.

3) The frequency of the peak spectral intensity and the coherence decrease toward the vortex core, while the frequency bandwidth and the peak intensity increase.

4) Autocorrelation peak broadens and time scale increases further downstream in the flowfield. The autocorrelation becomes dominated by the flow structures of interest; thus the frequency calculated from the autocorrelation matches the spectral peak.

5) The spectral peak originates along the leading edge at 30% span region (x'/c = 0.25). The origin was detected further upstream near the leading-edge region than the centerline.

6) The origin moves upstream with increasing angle of attack and decreasing sweep angle.

7) The trajectory of high coherence and intensity of quasiperiodic structures appears to follow a helical path. Coherence alone is not always a sensitive indicator to track an ensemble-averaged trajectory of the flow structures. The relative intensity of the spectral peak was used as a second indicator.

8) Convection speeds, based on the cross-correlation time shift, of the structures are generally near 50% of freestream speed, but do vary in the flowfield.

9) Fluctuation trends outlined above exist over an isolated delta wing and are not caused by tails, fuselage, strakes, inlets, or other flow obtrusions associated with an aircraft.

The following conclusions are made for the single point measurements:

1) The peak frequency scaled linearly with the freestream speed for all incidences tested. The product of the Strouhal number based on the semispan and the nominal wake scale was relatively constant over the Reynolds number range tested.

2) The absolute peak spectral intensity increases with increases in incidence or freestream speed, a probable effect of the strengthening of the shear layer. The nondimensionalized form of the spectral energy, however, generally decreases with increases in freestream speed.

Acknowledgments

This work is supported by the Air Force Office of Scientific Research, Dan Fant is the Technical Monitor. Special thanks are given to M. Klein, who conducted the single point measurements, and the students in the Experimental Aerodynamics Group.

References

[1]Colvin, B. J., Mullans, R. E., Paul, R. J., and Roos, H. N., "F-15 Vertical Tail Vibration Investigations," McDonnell Aircraft Co., MDC Rept. A6114, St. Louis, MO, Sept. 1979.

[2]Triplett, W. E., "Pressure Measurements on Twin Vertical Tails in Buffeting Flow," *Journal of Aircraft*, Vol. 20, No. 11, 1983, pp. 920–925.

[3]Wentz, W. H., Jr., and Kohlman, D. L., "Vortex-Fin Interaction of a Fighter Aircraft," AIAA Paper 87-2474, Aug. 1987.

[4]Lee, B. H. K., and Brown, D., "Wind Tunnel Studies of F/A-18 Tail Buffet," *Journal of Aircraft*, Vol. 29, No. 1, 1992, pp. 146–152.

[5]Washburn, A. E., Jenkins, L. N., and Ferman, M. A., "Experimental Investigation of Vortex-Fin Interaction," AIAA Paper 93-0050, Jan. 1993.

[6]Komerath, N. M., Schwartz, R. J., and Kim, J. M., "Flow over a Twin-Tailed Aircraft at Angle-of-Attack, Part II: Temporal Characteristics," *Journal of Aircraft*, Vol. 29, No. 4, 1992, pp. 553–558.

[7]Nelson, R. C., "Unsteady Aerodynamics of Slender Wings," *Aircraft Aerodynamics at High Angles of Attack: Experiments and Modeling*, AGARD-R-776, March 1991.

[8]Komerath, N. M., Schwartz, R. J., Percival, S., and Kim, J.-M., "Unsteady Vortex Flow Measurements over Twin-Tailed Aircraft at High Angles-of-Attack," AIAA Paper 91-0279, Jan. 1991.

[9]DeBry, B., Komerath, N. M., Liou, S-G., Caplin, J., and Lenakos, J., "Measurements of the Unsteady Vortex Flow over a Wing-Body at Angle-of-Attack," AIAA Paper 92-2729, June 1992.

[10]Klein, M. A., Hubner, J. P., and Komerath, N. M., "Spectral Measurements in Vortex Flow over Swept-Winged Configurations at High Angle-of-Attack," AIAA Paper 94-1804, June 1994.

[11]Rediniotis, O. K., Stapountzis, H., and Telionis, D. P., "Periodic Vortex Shedding over Delta Wings," *AIAA Journal*, Vol. 31, No. 9, 1993, pp. 1555–1562.

[12]Ashley, H., Rock, S. M., Chaney, K., and Eggers, A. J., Jr., "Active Control for Fin Buffet Alleviation," WL-TR-93-3099, Wright-Patterson AFB, OH, 1993.

[13]Mabey, D. G., and Pyne, C. R., "Buffeting on the Single Fin of a Combat Aircraft at High Angles of Incidence," *AAF International Forum on Aeroelasticity*, Vol. 1, Strasbourg, France, May 1993, pp. 223–241.

[14]Bendat, J. S., and Piersol, A. G., *Random Data: Analysis and Measurement Procedures*, 2nd ed., Wiley-Interscience, New York, 1986.

[15]Visser, K. D., and Nelson, R. C., "Measurements of Circulation and Vorticity in the Leading-Edge Vortex of a Delta Wing," *AIAA Journal*, Vol. 31, No. 9, 1993, pp. 104–111.

[16]Dixon, C. J., "Semi-Empirical Analysis of Vortex Breakdown with Aerodynamic and Buffet Effects," AIAA Paper 94-3483, Aug. 1994.

[17]Wentz, W. H., Jr., and Kohlman, D. L., "Vortex Breakdown on Slender Sharp-Edged Wings," *Journal of Aircraft*, Vol. 8, No. 3, 1971, pp. 156–161.

[18]Gad-el-Hak, M., and Blackwelder, R. F., "Control of Discrete Vortices from a Delta Wing," *AIAA Journal*, Vol. 25, No. 8, 1987, pp. 1042–1049.

[19]Payne, F. M., Ng, T. T., Nelson, R. C., and Schiff, L. B., "Visualization and Wake Survey of Vortical Flow over a Delta Wing," *AIAA Journal*, Vol. 26, No. 2, 1988, pp. 137–143.

[20]Lowson, V. L., "Visualization Measurements of Vortex Flows," AIAA Paper 89-0191, Jan. 1989.

[21]Reynolds, G., and Abtahi, A., "Three-Dimensional Vortex Development, Breakdown, and Control," AIAA Paper 89-0998, March 1989.

[22]Hubner, J. P., and Komerath, N. M., "Visualization of Quasi-Periodic Structures in a Vortex Flow," AIAA Paper 94-0624, Jan. 1994.

[23]Washburn, A. E., and Visser, K. D., "Evolution of Vortical Structures in the Shear Layer of Delta Wings," AIAA Paper 94-2317, June 1994.

[24]Bean, D. E., Greenwell, D. I., and Wood, N. J., "Vortex Control Technique for the Attenuation of Fin Buffet," *Journal of Aircraft*, Vol. 30, No. 6, 1993, pp. 847–853.